Journal of Chromatography, 550 (1991) 799–809
Elsevier Science Publishers B.V., Amsterdam

CHROMSYMP. 2231

Quantitative particle-size distributions by sedimentation field-flow fractionation with densimeter detector[a]

J. J. KIRKLAND* and W. W. YAU

E. I. DuPont de Nemours and Company, Inc., Central Research and Development, Experimental Station, P.O. Box 80228, Wilmington, DE 19880-0228 (USA)

ABSTRACT

Certain colloidal samples pose problems in obtaining accurate transformation of turbidimetric detector signals in sedimentation field-flow fractionation (SdFFF) to the desired particle concentration output. A densimeter detector shows promise in eliminating these problems. This device responds to changes in the density of sample components in the channel eluent. Accurate concentrations of sample particles are available directly without the need for detector-response transformation. Displaying the required signal-to-noise sensitivity for inorganic colloids, the densimeter appears to be a useful alternative to the turbidimetric detector for many SdFFF applications.

INTRODUCTION

Sedimentation field-flow fractionation (SdFFF) is a superior method for determining the size and size distribution of colloids [1–6]. Particles of widely differing types in the range of *ca.* 10–10 000 nm can be accurately characterized with high precision without the need for standards or calibration [1,4,5].

SdFFF separations are performed in a thin, open channel that rotates within a centrifuge [7,8]. Because of an imposed centrifugal force, particles that are heavier than the liquid mobile phase settle radially outward against the accumulation wall of the channel. Build-up of particles next to this wall is resisted by normal diffusion in the opposite direction. Therefore, because of lower diffusion and higher sedimentation rates, larger and heavier particles are forced closer to the accumulation wall. These larger particles are intercepted by slower laminar-flow flow streams next to the wall. They are then eluted from the channel after smaller particles that are intercepted by higher flow stream velocities further from the wall.

The resulting SdFFF fractogram is a record of the elution of particles as a function of time. Earlier eluting peaks correspond to lighter and smaller particles, followed by particles of increasing mass or size. Data extracted from this fractogram

[a] Presented in part at the *Chromatography Award Symposium for Professor John Knox, American Chemical Society Meeting, Boston, MA, April 25, 1990.*

0021-9673/91/$03.50

permits the calculation of the particle size and particle-size distribution of the colloid sample [1,4,6].

Standards are not required for the SdFFF measurement, as the method is based on known physical first principles. The analytical precision is excellent because of high resolution [9]. Just as important, SdFFF is capable of handling samples with a wide range of particle sizes by utilizing programmed force-field methods, whereby the force field is decreased systematically during the experiment. Exponential decay of the centrifugal force field has been found to be a convenient method of programming. With this approach, a plot of retention time *versus* log (particle size) produces a linear plot for precise quantification [4].

Turbidimetric detection using a UV–visible photometer or spectrophotometer generally has been used for sensing particles as they elute from an SdFFF channel [1–3, 5–8]. This detection method is satisfactory for many particle size measurements. It usually provides adequate sensitivity, is readily available and is convenient to operate. However, the light-scattering principle involved in turbidimetry creates a problem in particle-size determination. Large particles scatter light much more effectively than small particles. Therefore, the response of the turbidimetric detector is very non-linear with particle size differences. This effect is illustrated in Fig. 1. This shows a family of plots of scattering efficiency, Q_{sca}, *versus* the parameter ρ, which is a complex function of spherical particle diameter, the relative refractive index of the particle and the suspending liquid and the reciprocal of the wavelength of the imping-

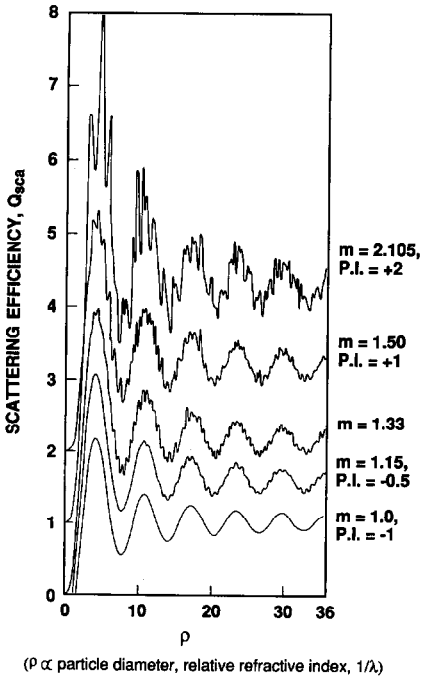

Fig. 1. Scattering efficiency plots for spherical particles. P.I. = plotting index; plotting scale change in scattering index units to simplify presentation. Adapted from ref. 10.

ing light. Here, $\rho = 2\pi d_p(m-1)/\lambda$, where d_p is the particle diameter, m is the relative refractive index ratio and λ is the wavelength of light in the medium. Plots are shown for various relative refractive index ratios, m (these plots are offset for ease of comparison). The initial steep portion of these plots represents the well known particle Rayleigh scattering regime. However, as ρ values increase (larger particles, higher refractive index, shorter wavelength), a complex "ringing" scattering function is found. The scattering function becomes extremely complex as the refractive index ratio m increases.

The complex scattering function shown in Fig. 1 greatly complicates the extraction of quantitative particle-size data from a turbidimetric detector output. Typically, this problem is handled by using computer software which transforms the turbidimetric detector output signal to true concentration values using the Mie scattering theory [11]. This approach generally provides good results, and so it is well suited and convenient for many applications.

However, experience has shown that turbidimetric detection is less desirable for measuring certain types of particles. Very small particles (*e.g.*, < 10 nm) are difficult to detect at useful concentrations because they scatter poorly. Decreasing the detector wavelength improves but often does not solve this problem. Another limitation is that the detector response to particles with high refractive indices is very difficult to convert accurately to concentration, as implied by the complex plots in Fig. 1. As a result, certain types of samples need a different type of detection to eliminate these problems, so that accurate particle-size information can be obtained.

This paper describes the application of a sensitive densimeter detector for determining particle size and particle-size distributions by SdFFF. This device, based on the mechanical oscillator method, directly measures particle concentration without any need for transforming the output signal. The detector also provides adequate sensitivity for inorganic colloids. Therefore, this device is a useful complement to turbidimetry in SdFFF particle-size measurements of colloidal materials.

EXPERIMENTAL

Apparatus and reagents

The SdFFF equipment used was the same as previously described [8,12]. A schematic diagram of the equipment is shown in Fig. 2. The densimeter detector was a Model DDS 70 (Anton Paar, Graz, Austria) prototype similar to that described by Trathnigg and Jorde [13]. The volume of the oscillator tube was 30 μl, and the total volume with the connecting tubing was 200 μl. This level of cell volume does not cause significant band broadening because of the relatively broad bands associated with SdFFF separations [3]. The temperature of the densimeter detector cell was maintained constant by placing it in a polyethylene bag located within a 20-l insulated foamed-polyethylene box filled with water. An inlet line of "crimped" 120 × 0.05 cm capillary tubing was loosely coiled around the detector cell within the bath to insure that the channel effluent entered the cell at the same temperature.

Colloid samples were obtained from DuPont. Scanning electron micrographs were obtained with a Model 840 instrument (Joel, Tokyo, Japan). Aerosol-OT was made from a 10% solution obtained from Fisher Scientific (Fair Lawn, NJ, USA). "Micro" detergent was obtained from Cole-Parmer Instrument (Chicago, IL, USA).

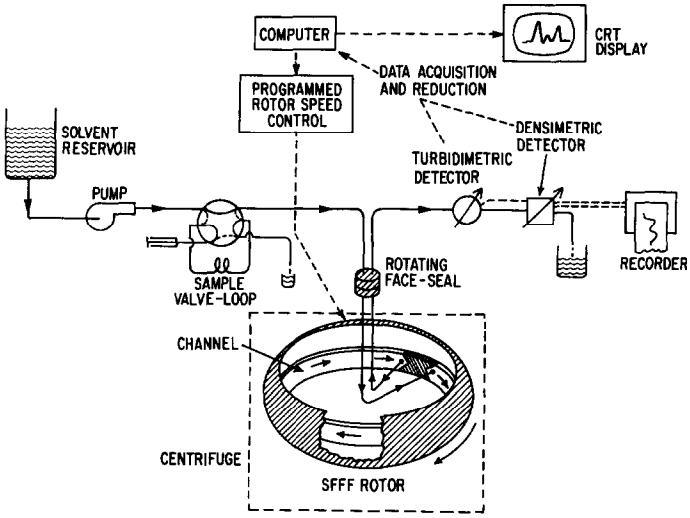

Fig. 2. Schematic diagram of sedimentation FFF apparatus with a densimeter detector.

Density detection

The basics of the densimeter detector using a mechanical oscillator were previously described by Trathnigg and Jorde [13]. The measuring cell contains an oscillating, U-shaped glass tube. Under optimum conditions, the oscillation period of this tube describes the density of its contents with precisions approaching 10^{-6} g/cm^3:

$$d = AT^2 - B \tag{1}$$

where d is the density of the material in the tube, T is the time period of the oscillation and A and B are constants for each cell. These constants are determined by a two-point calibration using water and air, or two solvents of widely different known densities. A density change Δd within the cell is then

$$\Delta d = A(T_2^2 - T_1^2) = A(T_2 - T_1)(T_2 + T_1) \tag{2}$$

where T_1 and T_2 are the initial and measuring time period of oscillations, respectively. For the small density changes measured in SdFFF,

$$T_2 + T_1 = 2T_0 \tag{3}$$

and

$$\Delta d = 2AT_0 \mathrm{d}T \tag{4}$$

or, substituting eqn. 1,

$$\Delta d = 2(B + d_0)(\Delta T/T) \tag{5}$$

where dT or ΔT is the change in the oscillation time period and d_0 is the density of the mobile phase liquid.

Now, the period T_m is determined by counting the number N_b of periods T_b of a standard time base (a 10-MHz quartz oscillator) within a measuring interval t_m for a constant number N_m of periods T_m of the measuring cell:

$$t_m = N_m T_m = N_b T_b \tag{6}$$

Combining eqns. 5 and 6 gives

$$\Delta d = 2(B + d_0)(\Delta N_b / N_b) \tag{7}$$

The mobile phase volume V passing through the cell within each measuring interval at flow-rate F is

$$V = F N_b T_b \tag{8}$$

This volume contains a mass m_i of a solute i to be measured, and this will cause a density change:

$$\Delta d = c_i(1 - d_0 V_i^*) = a_i m_i / V \tag{9}$$

where $a_i = 1 - d_0 V_i^*$ and V_i^* is the volume for each specific measuring interval. Combining eqns. 7–9 gives

$$m_i = 2T_b(B + d_0)(F/a_i)x_i \tag{10}$$

where $x_i = (\Delta N_b)_i$; the digital response of the density detector is integrated over each measuring interval t_m to determine the mass of solute eluted with t_m. Integration of a peak is performed by summing x_i.

RESULTS AND DISCUSSION

The utility of the densimeter detector in the measurement of the particle-size distribution of colloids is illustrated in Fig. 3 for a silica sol sample. These data were obtained using the time-delay, exponential-decay force-field programming method (TDE-SFFF) that has been described previously [4]. The left hand panels in Fig. 3 show the "raw" turbidimetric detector *vs.* time output and the relative concentration *vs.* linear particle diameter plot. The latter was obtained by transforming the "raw" detector signal using software containing the Mie scattering correction method [11]. Panels on the right in Fig. 3 show data obtained with the densimeter detector on a separation identical with that performed with the turbidimetric detector. In this case, no transformation of the "raw" detector signal was required, because the output of the densimeter detector is linear with sample concentration. As shown by the data in the lower panels in Fig. 3, results for this silica sol sample are closely similar for the two different detectors.

Limitations of turbidimetric detection for measuring the particle-size distribu-

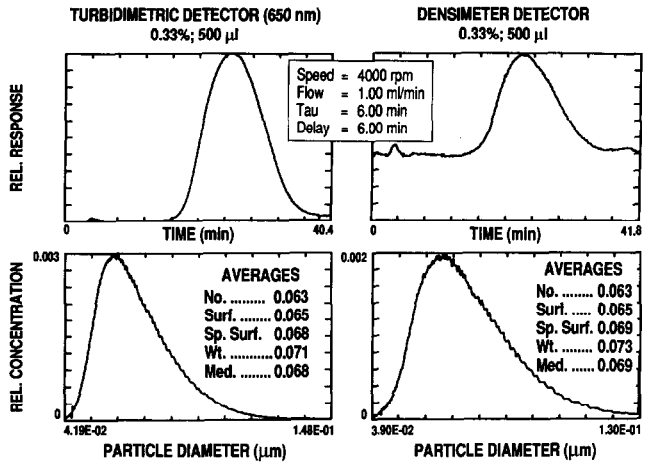

Fig. 3. Comparative detection for silica sol sample separated by TDE-SFFF. Mobile phase, 1 m*M* ammonia solution; ρ_S = 2.2 g/cm^3; $\Delta\rho$ = 1.2 g/cm^3; other operating parameters as shown.

tion of certain samples is illustrated in Fig. 4. The top panel shows the "raw" detector signal in a fractionation of a diamond dust sample. The middle panel represents the attempted transformation of the "raw" signal with the Mie scattering method to obtain the relative concentration or differential plot of concentration *vs.* particle size.

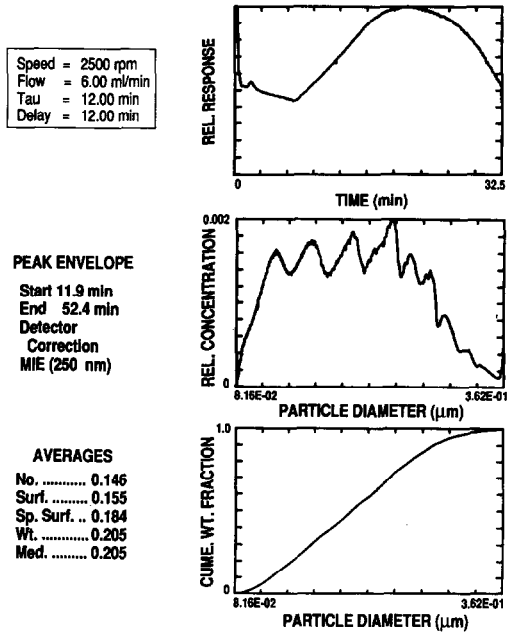

Fig. 4. TDE-SFFF of diamond dust with turbidimetric detection. Mobile phase, 0.2% "Micro" detergent; ρ_D = 3.51 g/cm^3; $\Delta\rho$ = 2.51 g/cm^3; detector, 250 nm; other operating parameters as shown.

The severe "ringing" effect seen in this plot is actually not characteristic of the sample, but results from errors in the transformation process. These errors arise from the very high refractive index of diamond and the relatively low wavelength (250 nm) used for the turbidimetric detection. These factors cause the scattering regime to be in a region that involves strong "ringing" or oscillations, as shown by the plots in Fig. 1. Small errors in refractive index, particle diameter or wavelength values for the transformation process then can create the type of "ringing" effect seen in the middle plot in Fig. 4, and also in the lower cumulative plot. This "ringing" effect also can cause errors in the calculation of particle diameters and particle-size averages for the samples.

As suggested by the plots in Fig. 1, increasing the wavelength of turbidimetric detection would place the scattering regime in a region where the "ringing" problem should be reduced. This is borne out by the data in the left-hand panel of Fig. 5. Here, the diamond dust sample now shows considerably less of the "ringing" effect in the differential plot when detection was performed at 700 nm, compared with 250 nm. Note that the calculated particle averages are smaller than those found at the higher detector wavelength.

Use of the densimeter detector for the diamond dust sample produced an unexpected bonus in measurement accuracy. The differential plot in the panel on the right in Fig. 5 shows a population of smaller particles that were not sensed by the turbidimetric detector under the conditions used. The reason for this is that the turbidimetric detector signal decreases as a fourth-power function of particle diameter (see Fig. 1). Again, transformation accuracy in turbidimetric detection is poor with very small particles. Note that the calculated averages with the densimeter detector are now significantly smaller, and in keeping with the manufacturer's claim of "1/8 μm" particles. In the scanning electron micrograph in Fig. 6, the presence of a population of <0.1 μm particles is apparent, in addition to particles <0.3 μm.

Comparison of turbidimetric and densimetric detection is also shown in Fig. 7

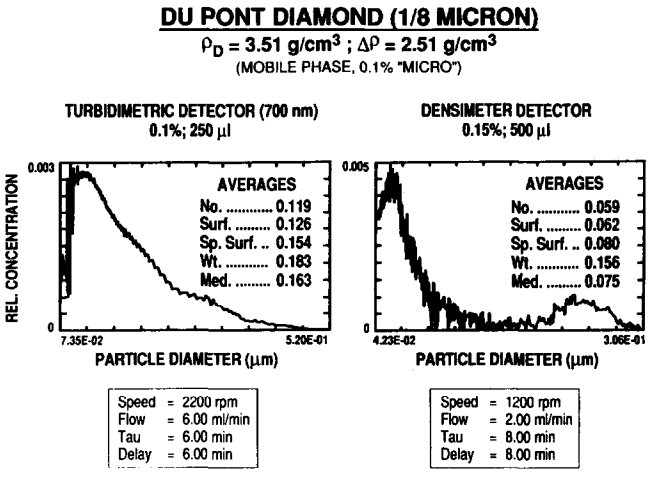

Fig. 5. Comparative detection with TDE-SFFF separation of diamond dust sample. Mobile phase, 0.1% "Micro" detergent; turbidimetric detection, 700 nm; other operating parameters as shown.

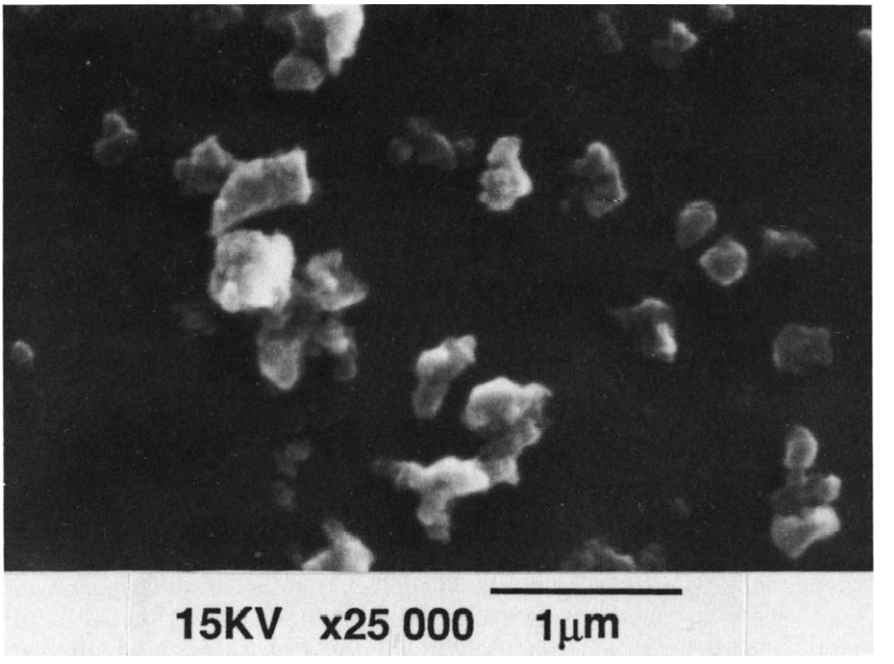

Fig. 6. Scanning electron micrograph of diamond dust particles.

in the particle-size distribution measurement of a chromium dioxide sample. "Raw" detector outputs and differential plots are shown for both detection systems. Excellent correlation was found for particle-size averages calculated for measurements with these detectors.

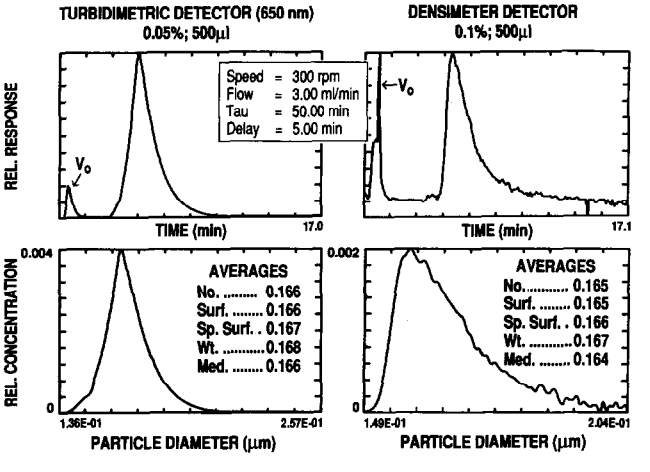

Fig. 7. TDE-SFFF of chromium dioxide. Mobile phase, 0.2% "Micro" detergent; ρ_{CD} = 4.86 g/cm^3; $\Delta\rho$ = 3.86 g/cm^3; other operating parameters as shown.

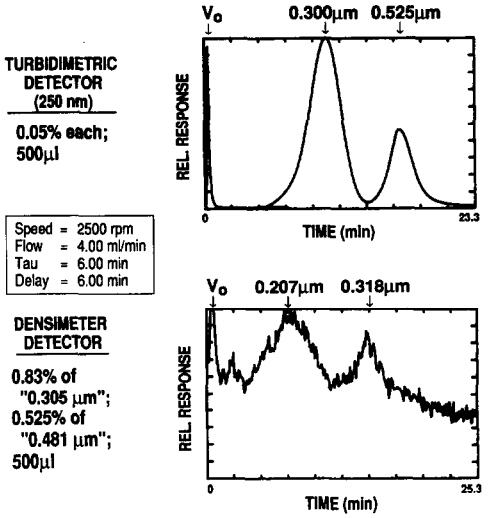

Fig. 8. Comparative detector sensitivity for polystyrene latex mixture. Mobile phase, 0.1% Aerosol-OT; ρ_{PS} = 1.05 g/cm^3; $\Delta\rho$ = 0.05 g/cm^3; other operating parameters as shown.

The main limitations of the densimetric detector in SdFFF applications involve inadequate sensitivity in instances where there are small differences in the densities of the particles and the mobile phase. The restriction is exemplified in Fig. 8 for the separation of two narrow-particle-size polystyrene latex standards (density of polystyrene = 1.05 g/cm^3; density of mobile phase = 1.00 g/cm^3; $\Delta\rho$ = 0.05 g/cm^3). The top graph shows the relative concentration *vs.* particle-size plot for the turbidimetric detector after transformation. The calculated values of 0.300 and 0.525 μm compare

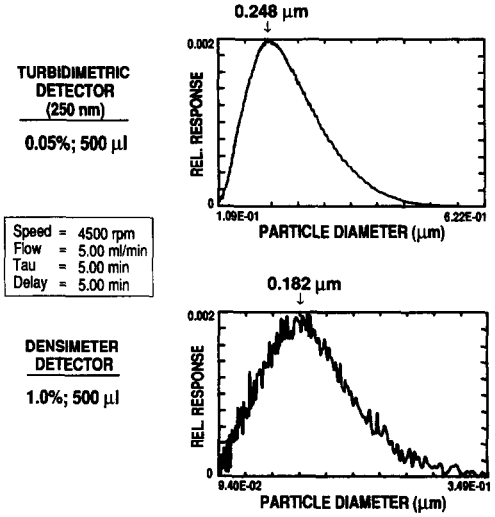

Fig. 9. Comparative detector sensitivity for experimental chloroprene latex. Mobile phase, 0.1% Aerosol-OT; ρ_N = 1.22 g/cm^3; $\Delta\rho$ = 0.22 g/cm^3; other operating parameters as shown.

with the supplier's values of 0.305 and 0.481 μm (the latter value is actually 0.535 $\pm$ 0.012 μm by independent measurements [14]). To obtain any recognizable signal with the densimeter detector (lower plate, Fig. 8), more than a 10-fold increase in sample concentration was required. Even at this high concentration, the detector signal was noisy. In this case, calculated values for particle sizes were significantly lower than actual, indicating that the channel was overloaded with sample. Overloading causes early elution of particles with resulting smaller than actual calculated values.

Organic polymer lattices with higher densities still do not give sufficient sensitivity with the densimeter detector to permit accurate analysis. This is illustrated by the data in Fig. 9 for a chloroprene (Neoprene) latex with a density of 1.22 g/cm^3 ($\Delta\rho$ = 0.22 g/cm^3). The top graph with the turbidimetric detector shows a peak-position particle diameter of 0.248 μm for this sample. With a 20-fold increase in sample amount, the densimeter detector signal (bottom plot) was still unacceptably noisy. The calculated particle-diameter value for the densimeter detector run was only about three quarters of that found with the turbidimetric detector, because of channel overloading.

CONCLUSIONS

The advantage of the densimeter in SdFFF analyses is that it is a universal detector needing no signal transformation for accurate particle-size distribution measurements. In its present form, the densimeter detector requires a density difference $\Delta\rho$ between the particle and the mobile phase of greater than 0.2 for adequate detection. Overloading the channel to compensate for inadequate signal-to-noise detector response results in particle-size measurements that are smaller than actual. Accurate particle-size distribution measurements are easily accomplished with densimetric detection if $\Delta\rho$ is greater than about 1.0. This means that this detector is well suited for measuring the particle size distributions of inorganic colloids by SdFFF, but has limited application for organic colloids that characteristically have lower densities.

The densimeter detector is sensitive to temperature, so the cell must be carefully thermostated. Incoming lines containing the channel effluent from the SdFFF should be thoroughly heat exchanged to minimize baseline upsets. As used in this study, the densimeter detector is essentially flow insensitive. This characteristic may make this device useful for flow programming in appropriate situations.

The densimeter detector used in this study has sufficient sensitivity for application in size-exclusion chromatography [13]. For general application in SdFFF for all types of colloids, an order of magnitude increase in sensitivity is needed, because of the significantly higher dilution of sample that occurs during the separation. Application of densimetric detection to thermal FFF and flow FFF would become highly attractive with increased sensitivity.

ACKNOWLEDGEMENTS

We thank W. H. Emerson for his assistance with the experiments and B. Trathnigg for his help in obtaining and setting up the densimeter instrument.

REFERENCES

1 J. C. Giddings, F. J. F. Yang and M. N. Myers, *Anal. Chem.*, 46 (1974) 1917.
2 F. J. Yang, M. N. Myers and J. C. Giddings, *J. Colloid Interface Sci.*, 60 (1977).
3 J. J. Kirkland, W. W. Yau, W. A. Doerner and J. W. Grant, *Anal. Chem.*, 52 (1980) 1944.
4 J. J. Kirkland, S. W. Rementer and W. W. Yau, *Anal. Chem.*, 53 (1981) 1730.
5 J. C. Giddings, K. D. Caldwell and H. K. Jones, *ACS Symp. Ser.*, 322 (1987) 215.
6 H. G. Mercus, Y. Mori and B. Scarlett, *Colloid Polym. Sci.*, 267 (1989) 1102.
7 J. C. Giddings, M. N. Myers, K. D. Caldwell and S. R. Fisher, *Methods Biochem. Anal.*, 26 (1980) 79.
8 J. J. Kirkland, C. H. Dilks, Jr. and W. W. Yau, *J. Chromatogr.*, 225 (1983) 225.
9 W. W. Yau and J. J. Kirkland, *Sep. Sci. Technol.*, 16 (1981) 577.
10 M. Kerker, *The Scattering of Light*, Academic Press, New York, 1969, p. 105.
11 G. Mie, *Ann. Phys.*, 25 (1908) 377.
12 J. J. Kirkland and W. W. Yau, *Anal. Chem.*, 55 (1983) 2165.
13 B. Trathnigg and C. Jorde, *J. Chromatogr.*, 241 (1982) 147.
14 W. W. Yau and J. J. Kirkland, *Anal. Chem.*, 56 (1984) 1461.